



Caroline Treib · Klara Loos · Michael Johlitz ·
Alexander Lion

Ozone ageing: experimental methods on pristine and protected natural rubber

Received: 26 March 2022 / Accepted: 18 August 2022
© The Author(s) 2022

Abstract Many industrial applications require natural rubber (NR) as an irreplaceable polymer for its unique behaviour as its resistance to crack growth. The damage caused by ozone, seen as an ageing accelerator, influences the lifetime of rubber components. The data on ozone-induced ageing experiments are often incomplete or remain unpublished, whereas comprehensive databases for other environmental loads as oxygen do exist. A variety of experimental methods is used to investigate the ageing mechanism of ozone. The ultimate scope is to collect physically based data suitable to include it in thermo-mechanical modelling of the material's full behaviour. Therefore, NR mixtures, without and with antiozonants: *p*-phenylenediamine (PPD) and paraffinic wax, are analysed. First, an accelerated, artificial ageing method is developed to reconstruct the real ageing in the laboratory. Experiments conducted henceforth are microhardness tests, uniaxial tensile tests and IR spectroscopy to determine the elastic modulus, the stress response and molecular change due to ageing. Independent of static deformation during the ageing process, both antiozonants show a significant protection effect up to the maximum loading with 75 pphm ozone concentration for 111 h at 50% relative humidity and 40 °C. Paraffinic wax completely prevents measureable mechanical change and no surface cracks are visible, though IR spectra reveal ageing-induced molecular reactions, whereas the pristine and solely 6PPD protected compounds are clearly distinguishable by their surface crack picture. Neither of the material compounds, loaded with or without strain during ozone-ageing, contains cracks of a depth further than 300 µm. The data generated on ozone ageing of rubber helps to distinguish it from thermo-oxidative ageing that is described comprehensively in the literature. In conclusion, the data proves the degradation and quantifies some characteristic material changes caused by ozone loading.

Keywords Ozone · Ageing · Natural rubber · Antiozonant · Experimental

Communicated by Andreas Öchsner.

C. Treib (✉) · K. Loos · M. Johlitz · A. Lion
Department of Aerospace Engineering, Institute for Mechanics, University of the Bundeswehr Munich,
Werner-Heisenberg-Weg 39, 85577 Neubiberg, Bavaria, Germany
E-mail: caroline.treib@unibw.de

K. Loos
E-mail: klara.loos@unibw.de

M. Johlitz
E-mail: michael.johlitz@unibw.de

A. Lion
E-mail: alexander.lion@unibw.de

1 Introduction

The range of applications of elastomers spreads into most areas of industry and everyday life. Natural rubber (NR), for example, is required in hoses, sealing, tyres, or isolators for bridges and motors. Several environmental loads affect the material characteristics temporarily or permanently during the lifetime, next to purely mechanical loads. Namely, environmental influences are temperature, UV-light, and humidity as well as surrounding media like oil, fuel, oxygen, and ozone or any combination of these. Economic and ecological interest in extended durability and prolonged service life rise due to raw material costs and customers requests, c.f. the works of [1,2].

Irreversible change in material characteristics strongly influences the service life and frequently is of chemical nature. The chemical change can be caused by gaseous or liquid surrounding media as ozone that permanently changes the characteristics of elastomers, as [3] points out. However, the literature still lacks experimental data dealing with ozonolysis in elastomers, recently claimed by [4]. In accordance with the claim, compared to other ageing mechanisms only few recent scientific publications deal with ozone-ageing of elastomers, as the research by [4–9]. In contrast, thermal and thermo-oxidative ageing is examined and understood in great detail, e.g. by [2,10–15].

A short overview follows regarding the publications specifically addressing ozone-ageing in rubber. Newton [16] is one of the first to describe separable effects of ozone loading on rubber compared to a combination with other environmental loads. Followed by a series of publications by [3,17–20] dealing with the cracks appearing in the embrittled surface layer: their initiation, growth and prevention by different antiozonants of which one is a type of *p*-phenylenediamine (PPD), still the most efficient type of antiozonant known. They describe the crack direction as orthogonal to the uniaxial, static force load applied as fixed weight. The crack growth of an initial flaw is said to be constant and independent of the level of stress as long as a critical stress value is exceeded. Rather the rate of crack growth is said to correlate mainly to the ozone concentration and the main polymer, the vulcanization system and the ageing protection chemicals [3]. However, Lake [21] states a dependency between the rate of crack growth and the strain applied regarding a stretched, cracked surface instead of one initiated flaw. Assessed by [19], a strain level from 0 to 30% strain leads to the evolution of increased surface roughness to fissures to macroscopic cracks. Before cracks appear, a gradient in stiffness over the sample depth can be assessed by so-called modulus profiling, as described by [22] for ozone-aged elastomers other than NR. Samples are cut to reveal their cross section, metallographically polished and the indentation depth of a tip entering the surface is measured. Musil [15] performed that procedure for thermo-oxidatively aged nitrile rubber on a metallographic microhardness tester with a Vickers indenter. In addition, Musil [15] conducted tension tests on layers of aged bars split after the ageing process to assess an ageing gradient in stiffness. Next to considerations on surface topology, modulus and macroscopic cracks, as well the chemical reaction of ozone and natural rubber has been analysed. The ozonolysis with alkenes is examined in detail by [23]. It is concluded that the cleavage of the double bond, which is as well found in the backbone of NR, see Fig. 1, is a three-step mechanism. In step 1 the ozone reacts in a 1,3-dipolar cycloaddition to the polymer chain and forms a primary ozonide. The unstable primary ozonide splits into a carbonyl and a carbonyl oxide in step 2 to recombine to a secondary ozonide in step 3. This secondary ozonide hydrolyses, oxidizes, reduces, thermolyses or photolyses to other final products like ketone derivatives when additional water is available [8]. This cleavage in step 2 manifests when mechanical strain is present, as [5] states and therefore is suspected to initiate further crack propagation on a microscopic scale. To assess a change in the molecular structure of NR, Zheng et al. [4] record FTIR spectra of the surface of pristine and aged NR samples. They show a significant difference that is attributed to the ageing mechanism.

At present, prevention of that chain scission is achieved by different antiozonants of which derivatives of PPDs are the most popular [24]. In addition, paraffin or microcrystalline waxes are used within the limit of static deformation. The two common antidegradants named are first a chemically protecting PPD that acts as a radical scavenger. Second, a physically protecting wax that forms up a non-reactive barrier according to [21]. Both antidegradants are of low molecular weight and migrate to the surface, as [24] states. Consequently their effect is dependent on the migration efficiency, thus, for example, temperature, degree of cross-linking and solubility, as described by [25]. Paraffinic wax can be rubbed off after migration in addition breaking the physical protection barrier. Limits of the known PPD antiozonants are pointed out by [26] to be, for example, dynamic strain conditions, high exposure temperatures, and discolouring as well as contamination of other surfaces. Though limitations are known, at present, PPD protects rubber still best, as stated by [5], who investigates the scavenging of ozone molecules by PPDs. Based on short ageing experiments up to 9 h

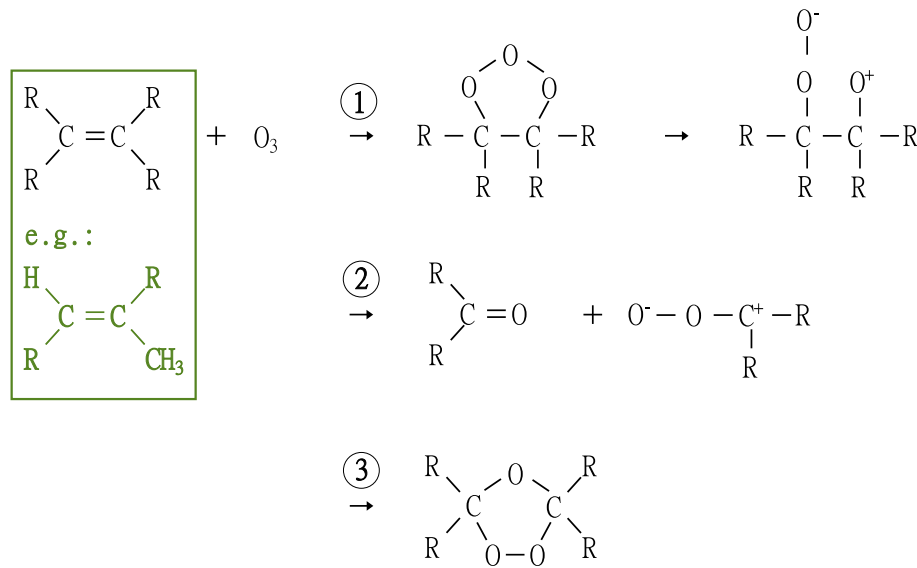


Fig. 1 Basic monomer of NR and Criegee's tree-step mechanism of ozonolysis [23]

Zheng et al. [4] develop a potential formulation for ozonolysis of NR. Besides this molecular change, ozone ageing is said to have a significant influence on tensile strength, specimen surface and cross-link density [4].

The following paper starts with a brief documentation on the NR compounds in use, the artificial ageing strategy applied and a description of the experiments' principles. The experiments cover uniaxial loading during ageing, a microhardness test, tensile tension testing and infrared spectroscopy. Ozone-induced change is detected as a crack pattern evolves, by crack depth and change in elastic indentation modulus over the sample thickness, stress distribution over the sample thickness and chemical change in the surface. Finally, the results are discussed regarding their antiozonant content.

2 Material and experimental methods

2.1 Natural rubber

The three investigated compounds have been manufactured by *The Centre of Polymer Systems of the Tomas Bata University Zlín, Czech republic*. Natural rubber is the main ingredient, supplied by *Thuan Loi Rubber Company Limited, SVR CV 60*, that consists almost completely of cis-1-4-polyisoprene. Figure 1 illustrates the monomer cis-1-4-polyisoprene with its typical double bond. It is filled with carbon black N330 from *Cabot Corporation* of particle size in the range from 26 nm up to 30 nm. Further, a sulphur (*Estman Chemical company*) vulcanization system with zinc oxide (*SlovZink*) and stearic acid (*Sigma-Aldrich*) is applied with the accelerator TBBS¹ (*Behn Meyer Europe GmbH, Perkacit*). The difference between the three compounds named *M1*, *M2*, and *M3* consists in the antiozonants added, cf. Table 1. Two antidegradants are chosen: on the one hand, the chemically protecting diamine 6PPD² (*Behn Meyer Europe GmbH, BEMOX*) and, on the other hand, a physically protecting paraffin wax (*Werba-chem GmbH*).

2.2 Artificial ageing strategy

NR degradation due to ozone needs to be properly reproduced artificially on shorter time scales in a laboratory, as by [9] or especially regarding DLO effects for thermo-oxidative ageing by [27]. NR ground-level ozone concentrations rise up to about 300 µg/m³ resp. 15 pphm³ ozone concentration, e.g. measured by German

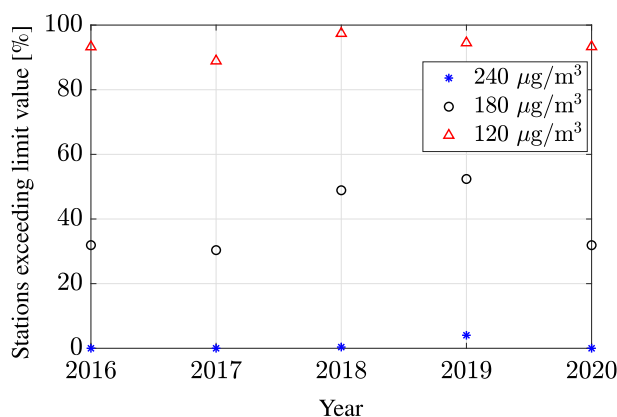
¹ *N*-tert-Butyl-2-benzothiazolesulfenamide.

² *N*-(1,3-dimethylbutyl)-*N'*-phenyl-p-phenylenediamine.

³ The measurements in environmental stations are given in µg/m³, whereas our laboratory devices use the pressure-independent unit pphm (volume fraction: parts per hundred million). At barometric pressure and 20 °C the units are associated by the factor 20.

Table 1 Composition of compounds

Component (phr)	<i>M1</i>	<i>M2</i>	<i>M3</i>
NR CV 60		100	
Carbon black N330		40	
Zinc oxide		3	
Stearic acid		1	
Accelerator TBBS		1	
Sulphur		2	
6PPD	3	3	0
Paraffin Wax	3	0	0

**Fig. 2** Percentage of meteorological stations in Germany that exceeded limit values of 120, 180, or 240 µg/m³ [28]

meteorological stations in the summer of 2019 [28]. Figure 2 counts the percentage of meteorological stations that have exceeded critical values of 120, 180, and 240 µg/m³ resp. 6, 9 and 12 pphm at least once within a year for the timespan 2016 to 2020. The alarm threshold of 240 µg/m³ resp. 12 pphm is not documented frequently at many stations in Germany. Nonetheless, even a few pphm ozone cause severe damage, claimed by [24], just as a high concentration within a shorter time scale. In addition, stationary meteorological stations cannot capture local accumulations of ozone clarified by their operators such as [28–30]. These accumulations arise due to supporting parameters such as high air pollution with volatile organic compounds.

To obtain reasonable ageing times, shorter than the full lifetime, acceleration is necessary. Two common adjustment parameters to speed up chemical processes are first, to increase the temperature or second to increase the concentration of the reaction partners. The temperature increase is the method applied in many thermo-oxidative research projects such as [14, 15, 31]. However, stable ozone concentrations can only be realized up to a temperature limit of about 60 °C, as stated by [32]. One reason for an upper temperature limit is that the current ozone concentration is the result of simultaneous production and decay processes. A temperature increase speeds up both processes to obtain the decay reaction running faster with increasing temperature than the production does. In addition, unintended chemical or physical reactions may run or even the ozone degradation process might change from the one at application temperature [11]. For the experiments conducted, a temperature of 40 °C is chosen, as proposed in the DIN standard [33]. Accelerated thermo-oxidative ageing is usually conducted at temperatures higher than 40 °C as in [14, 15, 31]. Thus, no strong acceleration is expected at 40 °C. However, ozone-induced changes will be compared to those from thermo-oxidative degradation by means of infrared spectroscopy in this contribution. As the ageing mechanism itself, the two antiozonants can be influenced by temperature in their migration behaviour. However, the service temperature of paraffin wax covers 40 °C and no significant change in the content of 6PPD was measureable in the outer 200 µm after ageing by a gas chromatography mass spectrometry analysis. Thus, the influence of the temperature is assumed to be neglectable at 40 °C.

To speed up the chemical processes of ozone ageing, the second possibility of an increase in the concentration of the reaction partner ozone is applied. In laboratory devices, the lowest feasible ozone concentrations

Table 2 Artificial ageing conditions applied in series 1 and 2

Component (phr)	Series 1	Series 2
Times (h)	4, 12, 48, 96	4, 12, 37, 111
Concentrations (pphm)	10, 20, 38, 75	25, 36, 52, 75
Static strain (%)	20	0, 20
Rel. humidity (%)	50	50
Temperature (°C)	40	40
Sample geometry	Bone-shaped	Bars punched from aged plates

**Fig. 3** Preparation of samples for microhardness indentation

named by manufacturers⁴ are 10 to 25 pphm ozone. Therefore, the lower limit for the range of ozone concentrations for artificial ageing coincides with the peak values of ambient measurements for ground-level ozone concentrations.

For the present study, two ageing series have been performed in sequence due to the availability of the ozone climate simulators used. The first series is aged with an ozone chamber of *Gibitre Instruments srl.* The second one with the device *SIM7500-TH* by *Anseros Klaus Nonnenmacher GmbH*. An overview of the ozone-ageing parameters applied is given in Table 2. The concentrations applied cover 10–75 pphm ozone at ageing times up to 111 h. The second series starts at 20 pphm in contrast to 10 pphm for the first series correlating with the given lower limits by the manufacturers of the two different devices. The achievable resolution of an in time ozone measurement is about 5 pphm according to *Anseros Klaus Nonnenmacher GmbH*. This differs to the measurements at meteorological stations that take at least 1 h. The applied ozone concentrations are up to 5 times higher than the maximal ambient concentration in order to accelerate the ageing process. However, the results are evaluated critically regarding possible changes in the chemical processes due to the acceleration. For both series the concentrations applied are logarithmically distributed between the lower limit and the maximal concentration of 75 pphm. Besides the ozone concentration, the ageing times of series 2 are also distributed logarithmically and cover a wider range from 4 to 111 h compared to the doubled ageing times up to 96 h in series 1. The influence of humidity on ozone degradation is examined by [7] with the result that for more than 50% relative humidity the degradation intensifies. Next to regular ozone attack water vapour reacts with ozone into hydroxy radicals that attack rubber in addition to pure ozone degradation similar to a degradation by ozonized water. Thus, the limit value 50% relative humidity is chosen as artificial ageing parameter. In the first series, all samples are aged at 20% deformation. The second series includes unstrained aged specimens in addition to strained ones. An important difference between the series is the order of ageing and sample punching. For the first series standard tensile bone-shaped specimens are vulcanized then aged. Thus, their edges are in a two-dimensional state. In contrast, for the second series samples are punched out of plates after ageing to obtain a one-dimensional ageing state.

2.3 Microhardness

Ageing due to ozone is based on a diffusion–reaction process depending on the diffusion rate as stated by [6]. Thus a gradient over the sample thickness establishes. The so-called *modulusprofiling*, introduced by [34], investigates a change in the elastic indentation modulus across the cross section of the sample, conducted by [22] on ozone-aged elastomers. Indentation tests are conducted using the microindenter by *Fischer GmbH*.

It is necessary according to [35] to perform a precise preparation of the specimen for the microhardness test. Further, Clough and Gillen [22] propose a metallographic preparation of the surface. Especially the surface

⁴ The here considered laboratory devices are ozone climate simulators by *Anseros Klaus Nonnenmacher GmbH* and *Gibitre Instruments srl.*

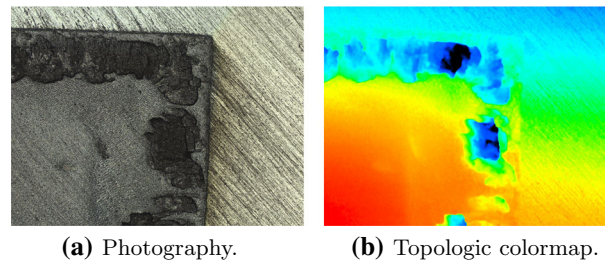


Fig. 4 Laser Scanning Microscopy—Cross section after microhardness preparation of compound *M2* after 96 h at 75 pphm ozone and 20% strain

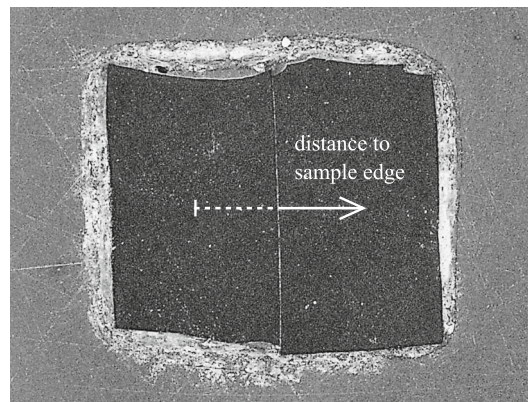


Fig. 5 Cross-section of prepared sample sandwich for modulus profiling

roughness of the cross section cut influences the measurement result, stated by [35]. Figure 3 illustrates the following description of the preparation conducted. In a first approach the bone-shaped rubber samples of series one are prepared alike the successful preparation of thermo-oxidative-aged elastomer samples by Musil [15]. The perpendicular cut rubber samples are stabilized for surface preparation and testing (A). The cut surface is embedded with the slow hardening epoxy resin set *EpoFix* by *Struers* (B). After hardening for 12 h, a polishing machine by *Struers* is used to reveal and smoothen the surface of the cross section (C). To avoid heating of the sample, the speed of the sandpaper disc is set to the minimum of 150 rpm (rounds per minute), the contact pressure to 5 N, and water is used to cool while grinding. Grinding papers of different grit sizes are applied successively: 320, 500 to 1200 grit size. After the preparation the rubber samples' cross sections are revealed (D, E).

Regarding the bone-shaped samples of series 1 containing cracks, the surface roughness is analysed additionally with a laser scanning microscope, see Fig. 4. The height differences in the surface layer reach 100 μm whereas the smooth looking centre has a surface roughness below 5 μm .

To determine the elastic indentation modulus, a Vickers indenter is used. The reproducible results are obtained in the specimen centre as in unaged specimen for the controlled test force of 50 mN. The resulting indentation depth in the sample centre is about 65 μm . The indentation depth is below the topologic height difference inside the ruptured part after grinding. But even at indenting with higher forces to increase the indentation depth, no reproducible measurement was possible in that surface layer.

Consequently, a second approach uses the unstrained aged plate samples of test series 2 without crack formation during ageing. These samples do not show any cracked surface layer nor the topology jumps in that edge area. Besides the disturbance of indentation measurements by the topology, the epoxy resin next to the sample can influence the result. For example, when the Vickers prism is touching the resin during the indentation process. In addition, the displacement is hindered even if the indenter is not in direct contact with the epoxy resin. Thus, the ozone-aged samples are embedded as a sandwich, cf. Fig. 5, so that the indenter can measure up to the surface of the sample without the influence of the surrounding epoxy resin.

A line of discrete points across the prepared cross section is measured perpendicular to the surface. Start and end point of the measured line are set at the samples' centres. The arrow from the edge towards the specimen centre depicted in Fig. 5 shows the starting point and the direction of the later displayed results that

are symmetrical to the common sample boarder. Beneficially, the epoxy resin is not influencing the indentation process and the force response with this method. The controlled test force is kept at 50 mN to obtain an indentation depth range comprising 40–65 μm depending on the material hardness at the measured point.

2.4 Tensile test

In order to quantify an ageing-induced stress profile, aged tension bars are sliced into layers of about 300 μm in thickness. The layers are cut using a *FBS AB320* precision band knife splitting machine by *Fortuna GmbH*. Adjustable distanced rollers transport the specimen towards and through the band knife. The accuracy of the upper roller is 0.05 mm of the lower one 0.01 mm, thus hardly any pressure is induced by the rollers. In addition, heating of the rubber while cutting is prevented by a lubricant containing water, liquid soap and isopropyl. Before slicing, the used standard bone-shaped tensile bars have a rectangular cross section of 4 mm times 2 mm. Subsequently, the layers are deformed at a constant rate of 0.0167 s^{-1} until total rupture or reaching 600%.

2.5 Infrared spectroscopy

To characterize chemical changes in the surface of the rubber compounds, Fourier transform infrared spectrometer (FTIR) spectra are recorded. They are conducted with an attenuated total reflectance (ATR) attachment '*Platinum ATR*' by *Bruker* in connection with the '*Tensor 27*' model. The range of wavelength is 400–4000 cm^{-1} with a resolution of 4 cm^{-1} . Each measurement consists of 32 scans. After the artificial ageing, the samples were vacuum-packed and stored in the fridge to avoid further ageing influences.

3 Results and discussion

3.1 Crack pattern after artificial ageing

After artificial ageing all strained samples without wax have developed visible cracks perpendicular to the strain direction (see Figs. 6, 7). This is in accordance with the works of [9, 17, 19].

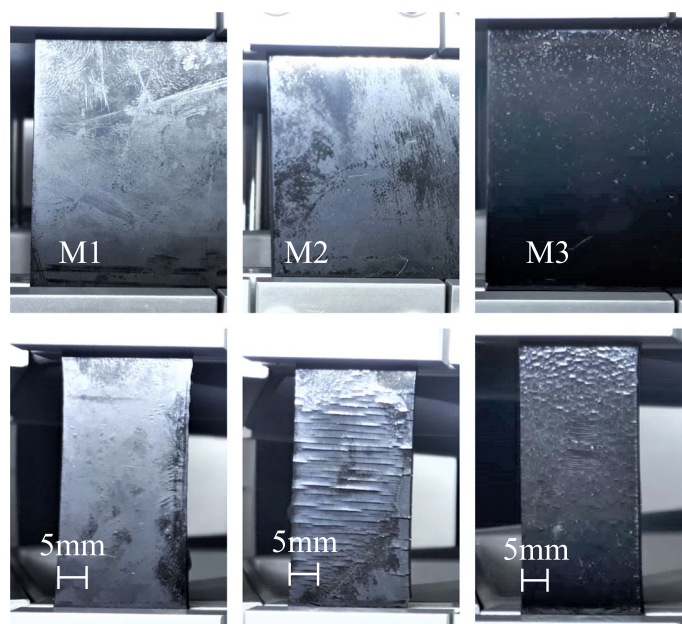


Fig. 6 Plates samples—surface after ageing for 111 h at 75 pphm ozone with (lower row) and without (upper row) tensile strain during artificial ageing

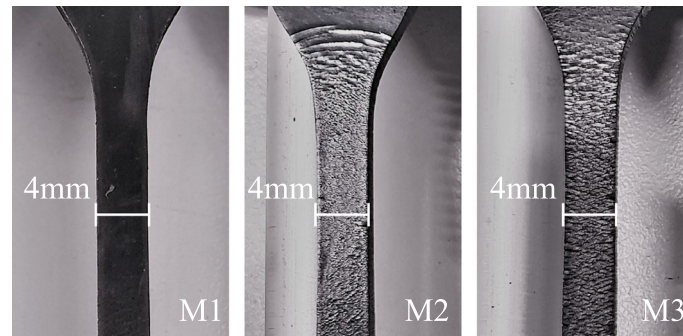


Fig. 7 Bone-shaped samples—surface after ageing at 20% deformation for 96 h at 75 pphm ozone

The second series of ageing, including both strained and unstrained plate samples, shows the strong effect of strain during ozone loading, cf. Fig. 6. The upper row shows photographs of the samples aged without mechanical load at 75 pphm ozone for 111 h. In the lower row, all samples have been deformed by 20% during identical ozone loading. Figure 7 depicts images of the first series of bone-shaped bars strained 20% during 96 h at 75 pphm ozone. Apparently, only if tensile stress is present, cracks evolve during the ageing, coherent with the results of [19] a minimal strain is necessary for cracks to evolve.

Similar crack patterns of different intensity are obtained for all tested ageing states. In contrast to the strain, varying ageing time and ozone concentration seem not to influence the crack characteristic for each of the three different compounds *M1*, *M2* and *M3*.

The compound *M1*, containing both a chemical protectant and a paraffin wax, shows no cracks visible by eye, independent of any static or dynamic deformation during ozone loading. The other two compounds develop cracks in the stretched configuration that differ in size and number. Numerous fine cracks cover the surface of *M3* without ageing prevention additives. Compared to that, the cracks in compound *M2* are less numerous but larger in size for the plate sample as for the bone part of the bone-shaped sample, whereas the middle part of the bone shows similar cracks compared to that of compound *M3*. At the bone part as in the plate, lateral contraction is hindered increasingly towards the clamping edge. In contrast, the centre of the bone-shaped sample faces no contraction constraint. We assume a strong correlation between strain and crack pattern to be analysed in more detail in further studies.

Compound *M1* and *M2* lose their glossy-looking surface that is kept by *M3* even after ageing. Thus, the change in the optical properties of the surface is attributed to the migration of 6PPD and paraffin wax. Furthermore, the glossy surface of compound *M3* after ageing is sticky as mentioned in [9]. The thermo-oxidative ageing study of [10] correlates a similar observation to an initial fast chain scission forming low molecular weight products resulting in a change in crosslink density further affecting the diffusion.

Visual cracks are the basis of standards such as [33] to classify ozone resistance. However, this solely visual approach is questionable. First, as diffusion takes place changes may occur even without mechanical loading and without visible cracking. Second, only the crack size but not the depth are assessed.

3.2 Crack depth

After the first approach of embedding the strained aged samples for the microhardness test, their cross sections of about one and two-millimetre side length have been viewed by optical microscopy. Exemplarily, enlarged pictures of the ageing condition of 96 h at 75 pphm ozone of all three compounds are presented in Fig. 8.

Whereas both compounds without wax, *M2* and *M3*, show a visual irregularity from the surface towards the centre, compound *M1* containing wax shows no change visible by optical microscopy. The identified optical spread in Fig. 8 can be attributed to the topologic height differences seen in Fig. 4. This observation is consistent over all ageing states at different depths of the irregular layer. The surface layer of *M2* differs from *M3* in the homogeneity of the boundary between surface layer and centre part of the cross section. *M2* protected with 6PPD seems to promote a smoother lateral increase of the boundary in contrast to unprotected *M3*. Compound *M3* shows a patchy progress from the surface inwards to the sample centre with a degraded layer depth extending up to 358 μm . A possible reason might be the gradient based migration of the 6PPD. It migrates faster the higher the concentration gradient is, thus faster to locations where more antiozonant is

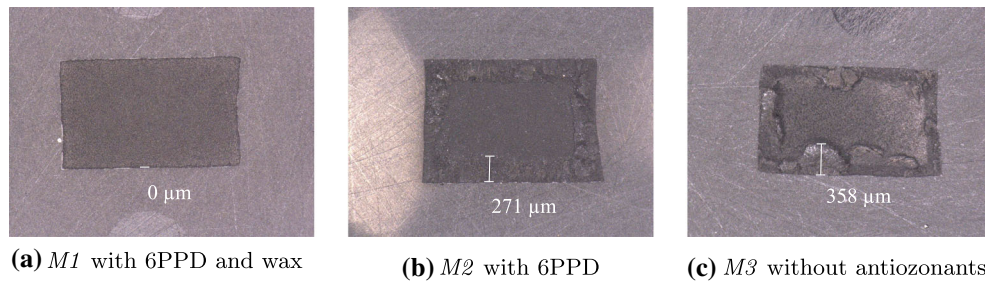


Fig. 8 Deteriorated surface layer visible on grinded cross section after 96 h at 75 pphm ozone

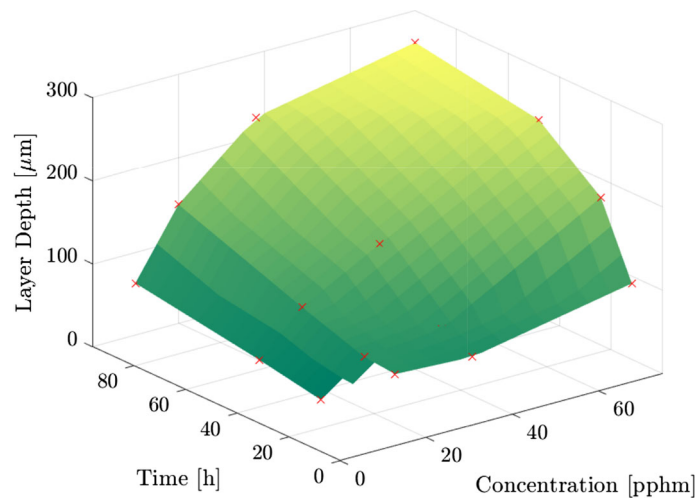


Fig. 9 Surface layer depth measured by optical microscopy of the cross section (red crosses) for compound *M2* aged under 20% static strain

consumed. Consequently, a homogenizing effect on the crack layer development is attributed to the use of the migrating antiozonant.

Since only the surface layer of compound *M2* is homogeneously in depth, Fig. 9 shows the evaluation of the surface layer growth of *M2*. For each ageing condition of series 1 the surface layer depth is plotted in z-direction. The y-axis is the concentration of ozone and the x-axis the corresponding ageing time. A regression surface visualizes the growth between the distinct points of ageing states. Thus it can be seen that the degraded or cracked surface layer of compound *M2* grows with ageing time as well as with ozone concentration. The layer depth seems to settle at a maximal value close to 300 μm under the most intense ageing conditions of series 1. In contrast, a steep change in layer depth is observed for less intense conditions. Regarding the ageing time, a network relaxation at constant strain reduces the present stress in the sample and therefore might slow down the crack growth rate. But the settling layer depth with rising concentration cannot be explained by a network relaxation. Possible reasons could be a lack of reaction products in terms of available rubber chains on the surface in addition to deposited reaction products hindering the diffusion.

Since the layer depth for compound *M3* is irregular as depicted in Fig. 8, an increase in depth cannot be measured. However, the maximum depth is about 30% higher than for compound *M2*. Regarding *M1* no surface layer can be identified.

3.3 Elastic indentation modulus

The unstrained ozone-aged samples of about 1.5 mm thickness show an influence of the oxidation on the indentation modulus. Towards the sample surface, the rise in the indentation develops abruptly. The samples shown exemplarily in Fig. 10 are of compound *M2* and aged under 25 pphm ozone concentration for different times. The depth, until a constant modulus similar to the unaged material is measured, comprises only 200 μm for the longest ageing time. The migration efficiency of the 6PPD added seems to be not fast enough to ensure

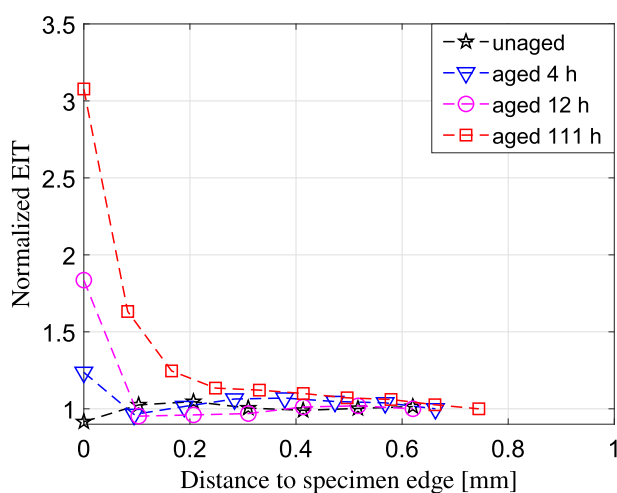


Fig. 10 Modulus profiling for ozone-aged NR specimens based on the normalized indentation modulus (EIT) for 25 pphm ozone concentration at different ageing times

a full protection. However, the ozone influence reaches a limit depth which might be caused by a diffusion-limited oxidation (DLO) effect as it is known for thermo-oxidative ageing [12, 15, 31] caused by a surface layer consisting of reaction products changing crosslinks and density [10]. For compound *M1* and compound *M3* no data is available yet for the sandwich approach. However, compound *M2* seems to be the most suitable for the testing method since for compound *M3* an irregular ageing depth is to be expected and compound *M1* might not show changes without strain during ageing.

In conclusion, the challenge of evaluating the ozone-aged samples is to grind the surface without tearing pieces of the most interesting part close to the aged surface. Since the microhardness test needs a surface preparation so that the indentation depth is small compared to the surface roughness, the microhardness test of the preloaded specimens failed. However, the layer depth that is deteriorated at the preparation process correlates with the ageing state. An attempt to explain the observed change close to the surface is that the existing cracks, cf. Fig. 7, are torn off during the grinding process.

A clear influence of the ozone ageing is given by the results of the microhardness tests on the unstrained aged specimens of compound *M2*. Some change in modulus is measured up to a depth of 200 μm . The rise in the indentation modulus is steep inside of that 200- μm -thick layer. For up to 12 h ageing time, the change in the elastic indentation modulus occurs in a thin surface layer about only 100 μm , as described by [22] for different elastomers. But the modulus in the centre is not changed by ozone ageing at all. Thus, a DLO effect seems to block further diffusion of ozone into the material completely.

3.4 Distribution of tensile stress over the thickness

The results of the tension tests are shown exemplarily in Fig. 11a for compound *M2* after stretched ageing for 95 h at 75 pphm ozone concentration. Whereas the layers in the centre show an equal stiffness behaviour, the outmost layers drop in stiffness as they change in shape. The start of a typical S-shaped curve for NR can be seen in Fig. 11a only for the centre layers. Compared to an unaged specimen, they do not differ significantly. In the outmost layers, the stress increases approximately linear.

Similar results are obtained for compound *M3* but more pronounced. In contrast to compound *M1* that does not show any difference in the outmost layer compared to the centre ones. As expected, the absence of any antiozonant leads to in the most severe degradation. Additional 6PPD moderates the degradation effect of ozone load at static deformation that seems to be completely prevented by paraffin wax.

Figure 7 shows that cracks cover the samples' surfaces for compound *M2* and *M3* after ageing. Therefore, cracks are immediately visible cf. Fig. 11b in the outmost layers at tensile deformation. Thus, even before the tensile test starts, their effective cross section is reduced. Respectively, the nominal stress must reduce as well.

The tensile test confirms the microscopic findings with regard to the degradation depth, cf. Fig. 9. A significant change in the stress–strain behaviour is measured only in the outmost layers thinner than 300 μm .

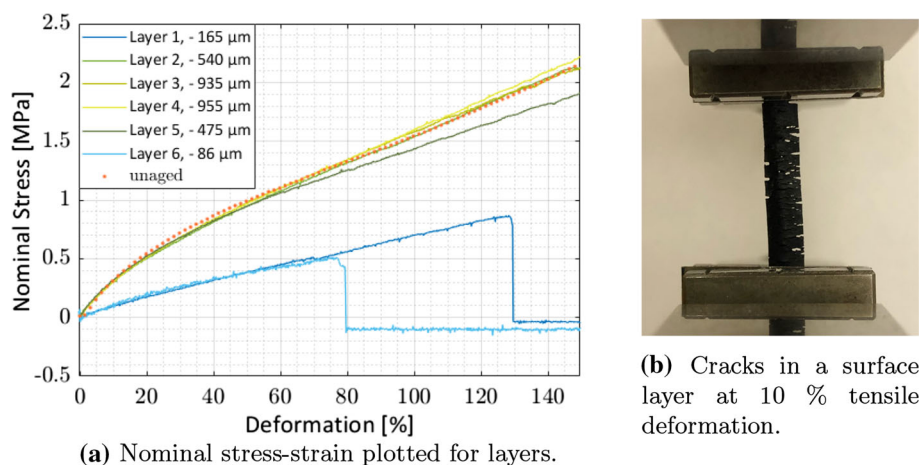


Fig. 11 Layers of a tension bar of compound M2 after 96 h at 75 pphm ozone concentration under 20% strain

No tensile tests of layers of the unstrained aged samples of series 2 have been conducted. The microhardness test for these specimens showed a pronounced change in the modulus at a maximal distance of 100 μm from the surface. Since the splittable layer depth is about 300 μm solely a change of the outmost layer is to expect. Other methods, for example, DMA testing might be promising to assess a stiffness increase in the surface of unstrained aged samples.

However, from the tests conducted two conclusions can be drawn in consistency with the microhardness: First, exclusively the outmost layer of less than 300 μm thickness shows a diverging stress level and evolution in comparison with an unaged sample. Second, the stress in the sample centre is not affected by the artificial ozone ageing conducted.

3.5 Chemical change in surface

The change in IR spectra for different ageing agents at 40 $^{\circ}\text{C}$ are compared in Fig. 12. IR spectra are depicted for the surface of compound M3 loaded thermo-oxidatively versus ozone both for a time of 111 h. In addition, the IR spectrum of a pristine sample is given. The slope of the resulting spectra differs strongly for the ozone loaded specimen, whereas pristine and thermo-oxidatively aged specimen show a similar gradient. Both aged samples show a peak development at around 1740 cm^{-1} typically corresponding to carbonyl groups according to [36]. Furthermore, only the thermo-oxidatively aged sample develops two peaks close to 1000 cm^{-1} . They do not appear for the ozone loaded sample assuming a suppression of thermo-oxidative reaction by the higher reaction rate of rubber with ozone. However, some reaction of rubber and oxygen takes place at 40 $^{\circ}\text{C}$ as the peak development close to 1000 cm^{-1} and around 1740 cm^{-1} indicates. In conclusion the temperature chosen for artificial ageing cannot guarantee any influence of oxygen or temperature but a dominating influence of ozone on the ageing process is most likely.

Figure 13 shows the IR spectra of the three compounds each unaged and aged for 111 h at 75 pphm ozone concentration without simultaneous strain. Low molecular weight components as the antiozonants may have migrated to the surface during artificial ageing as chain scission might have lowered the molecular weight of surface rubber molecules. Therefore, the samples were not touched except for the vacuum packaging nor cleaned to avoid any abrasion on the surface. Comparing the spectra of the unaged samples the absorption peaks of the main polymer branches are present in all three compounds.

According to [36] the backbone polymer peaks are assigned to stretching vibrations of polymer branches listed in Table 3. In the range of 1660 to 1740 cm^{-1} many oxidized side groups vibrate. Especially stated as ozonolysis product by [4,23], carbonyl compounds arise due to disruption of vinyl groups. The aged unprotected compound, M3, shows a strong peak at about 1740 cm^{-1} in response to the IR waves excitation. An increase in C–C and C–O bonds is assigned to the vibration peak at 1600 cm^{-1} after [36] given for M1 and M2 after ageing. As well observed by [4], this peak is assigned to stretching vibrations of the group C=C–C=C. The vibration bands at 1518, 1500, and 1320 cm^{-1} , present after ageing compound M1 and more pronounced in compound M2, indicate migration of the antiozonant 6PPD to the surface during the ageing process. The lower

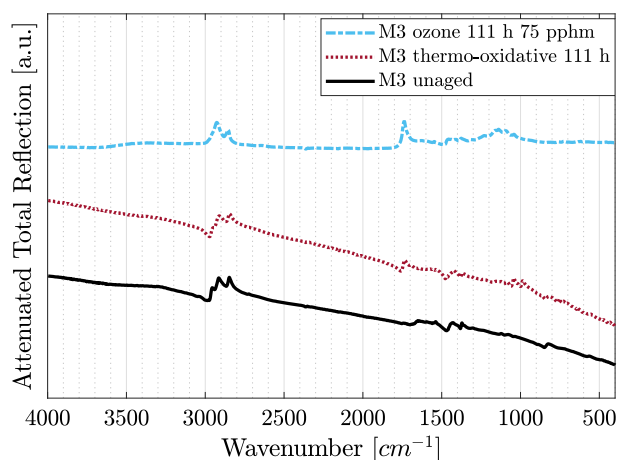


Fig. 12 Comparison of IR-spectra of the unaged, thermo-oxidative and ozone- aged surface of compound *M3*

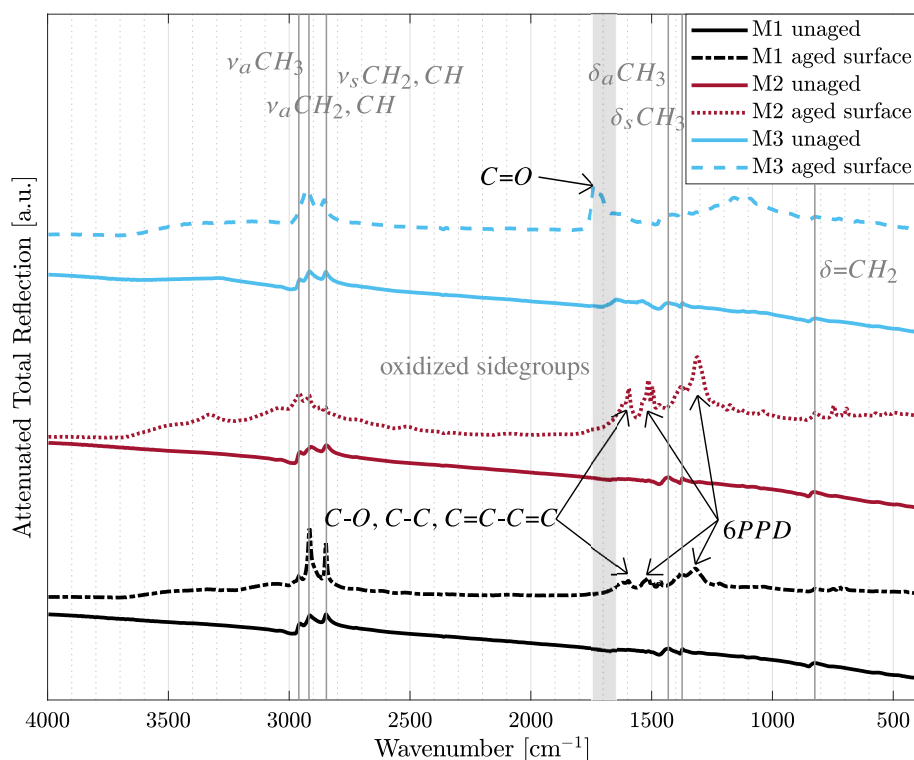


Fig. 13 Normalized IR-spectra of the surface of compound *M1*, *M2*, and *M3* before and after ageing

intensity of peaks correlating to 6PPD is consistent with the theory of a thin, stretchable, and protective layer, formed by migration of wax to the surface, formulated by [21].

Even the compound *M1*, not showing any cracks or gradual change in indentation modulus over its cross section, clearly changes its IR-spectra on the surface after ageing, as both other two compounds do. The main polymer branches remain but change their intensity, thus quantity. An antiozonant-dependent chemical reaction affects the molecular structure including some change of characteristic side groups. Only the unprotected NR, *M3*, forms carbonyl compounds as proposed by [8] whereas 6PPD seems to hinder further reaction steps after $C=C-C=C$, $C-C$ and $C-O$ are built.

Table 3 Stretching vibrations of polymer branches assigned to wavenumbers according to [36]

Wavenumber	Polymer branch
2962 cm ⁻¹	ν_a CH ₃
2920 cm ⁻¹	ν_a CH ₂ , CH
2850 cm ⁻¹	ν_s CH ₂ , CH
1370, 1435 cm ⁻¹	δ_a CH ₃ , δ_s CH ₃
825 cm ⁻¹	δ =CH ₂
1660 to 1740 cm ⁻¹	oxidized side groups
1740 cm ⁻¹	C=O ^b
1600 cm ⁻¹	C–C, C–O, C=C–C=C ^a
1518, 1500, 1320 cm ⁻¹	6PPD

^aStated by [4]^bStated in addition by [4,23]

3.6 Discussion

The conducted tests detect and quantify changes due to ozone exposure of pristine and ozone-aged NR. Pristine NR rubber is compound *M3*, whereas *M2* contains 6PPD and *M1* additionally contains paraffin wax. After unstrained ozone ageing, compound *M3* shows a glossy, sticky surface that is attributed to low molecular weight reaction products of the ozonolysis that both protected compounds do not show. Furthermore, the crack pattern varies strongly with the local residual stress, except for compound *M1*. Paraffin wax seems to protect well enough such that cracks cannot initiate for the unstrained and statically strained artificial ageing. The specimens of compound *M2* and *M3* are clearly distinguishable from each other on the basis of their crack patterns. *M3* shows numerous fine cracks, contrary to less but longer cracks for *M2*. A height difference in a surface-close layer has been exposed by metallographically grinding the cross section of specimens that have been stretched during artificial ageing. For the compound containing the chemical antiozonant 6PPD that layer is of constant thickness indicating a homogenous ageing resp. crack depth. In contrast, without 6PPD an irregular ageing boarder is observed. This correlates well with the crack pattern that shows long cracks for *M2* but for the inhomogeneous layer of *M3* numerous small cracks. Additional paraffin wax does completely prevent any visual surface layer. The difference between *M2* and *M3* might be caused by the gradient based migration of the antiozonant 6PPD that selectively supplies spots where it is consumed better than others. The maximal degradation depth, measured from microscopic pictures of the cross section, seems to settle for all strained aged samples. Except for the compound *M1* that shows no degradation layer. On the one hand, a network relaxation might cause a decelerated crack growth with ageing time. On the other hand a diffusion hindering layer might evolve with time as with increasing concentration, leading to a crack depth settling. Modulus profiling shows a steep rise in indentation modulus towards the sample surface even for chemically protected NR after ageing. The depth reaches 200 μm after which the change subsides until no change is measurable in the sample centre. The centre modulus is alike the unaged reference indicating a pronounced DLO effect. As well tension tests on layers show a constant stress distribution in the sample centre similar to that of the unaged material regarding all three compounds, whereas the outmost layers affirm a degraded surface for *M2* and *M3* of a depth below 300 μm . Finally, though paraffin wax seemed to hinder all changes described ahead IR spectroscopy reveals a chemical change in the surface of compound *M1*. Even without strain during ageing, chemical change of the specimens' surface is affirmed by the measured IR-spectra for all compounds. In unprotected natural rubber the evolution of carbonyl groups indicates oxidation on the surface. In the protected compounds the migration of 6PPD to the surface is visible in the spectra. The unaged state shows little difference in the spectra between all three compounds having no pronounced antiozonant peaks.

4 Conclusion and outlook

The present study analyses the ageing mechanism of ozone using a variety of experimental investigations. The three NR mixtures investigated differ in the application of antidegradants, 6PPD and paraffin wax. The approaches conducted reveal the susceptibility of NR even if these antiozonants are present. In the unstrained aged samples a steep change in modulus is present declining towards the bulk that is similar to the pristine samples. This is indicating a strong DLO effect supported by the tension tests that show no change for the

centre layers of the specimen after ageing. The compound containing wax does not show any change in modulus nor cracks; however, IR spectroscopy reveals chemical change on the surface has happened during ageing indicating the migration of lower molecular weight antioxidants. Preparation of strained aged samples metallographically revealed surface layers for the compounds without wax. The use of 6PPD leads to a homogenous layer in contrast to the unprotected compound with a patchy progress from the surface to the bulk. The chemical antioxidant should migrate to the location of highest consumption and thus smoothen the ageing front to be more homogeneous than without it. As well in the crack pattern the difference is visible between the compound without antioxidants and the one including 6PPD by number and size of cracks appearing lateral to the strain direction. The crack depths for strained aged specimen seem to settle at rising ageing time and concentration for the applied strain. Whether that maximal degradation depth is independent of the size of strain during the artificial ageing is to be analysed by upcoming experiments. Thus, further investigations are necessary to quantify the characteristic change in material behaviour. It is proposed to include different static strain levels during the artificial ageing procedure as well as dynamic deformation to generate a deeper understanding of the correlation between degradation, mechanical load and correlating crack patterns regarding, e.g. distribution, size or angle of the cracks. To gain insight in the change of the elastic modulus as well as the elongation at break further tension experiments are considered. A next attempt is to first split specimens into layers to afterwards age them and conduct uniaxial tensile tests. Another attempt could be to analyse the stiffness change in unstrained aged samples without cracks by means of DMA. As well only IR spectra of the surface have been conducted that shall be extended by lateral measurement lines through the cross section with IR microscopy.

Acknowledgements Parts of this research paper are funded by dtec.bw—Digitalization and Technology Research Center of the Bundeswehr which we gratefully acknowledge [Project FLAB-3Dprint].

Open Access This article is licensed under a Creative Commons Attribution 4.0 International License, which permits use, sharing, adaptation, distribution and reproduction in any medium or format, as long as you give appropriate credit to the original author(s) and the source, provide a link to the Creative Commons licence, and indicate if changes were made. The images or other third party material in this article are included in the article's Creative Commons licence, unless indicated otherwise in a credit line to the material. If material is not included in the article's Creative Commons licence and your intended use is not permitted by statutory regulation or exceeds the permitted use, you will need to obtain permission directly from the copyright holder. To view a copy of this licence, visit <http://creativecommons.org/licenses/by/4.0/>.

References

- White, C.C., White, K.M., Pickett, J.E. (eds.): Service Life Prediction of Polymers and Plastics Exposed to Outdoor Weathering. Matthew Deans (2018)
- Zaghoudi, M., Kömmling, A., Jaunich, M., Wolff, D.: Oxidative ageing of elastomers: experiment and modelling. *Contin. Mech. Thermodyn.* 1–9 (2022). <https://doi.org/10.1007/s00161-022-01093-9>
- Braden, M., Gent, A.: The attack of ozone on stretched rubber vulcanizates. I. The rate of cut growth. *J. Appl. Polym. Sci.* **3**(7), 90–99 (1960)
- Zheng, T., Zheng, X., Zhan, S., Zhou, J., Liao, S.: Study on the ozone aging mechanism of natural rubber. *Polym. Degrad. Stabil.* **186**, 109514 (2021). <https://doi.org/10.1016/j.polymdegradstab.2021.109514>
- Cataldo, F.: Early stages of p-phenylenediamine antioxidants reaction with ozone: radical cation and nitroxyl radical formation. *Polym. Degrad. Stabil.* **147**, 132–142 (2018)
- Früh, A., Egelhaaf, H.J., Hintz, H.: PMMA as an effective protection layer against the oxidation of P3HT and MDMO-PPV by ozone. *J. Mater. Res.* **33**(13), 1891–1901 (2018)
- Iwase, Y., Shindo, T., Kondo, H., Ohtake, Y., Kawahara, S.: Ozone degradation of vulcanized isoprene rubber as a function of humidity. *Polym. Degrad. Stabil.* **142**, 209–216 (2017)
- Cataldo, F.: Protection mechanism of rubbers from ozone attack. *Ozone Sci. Eng.* **41**(4), 358–368 (2019)
- Kamaruddin, S., Muhr, A.H.: Investigation of ozone cracking on natural rubber. *J. Rubber Res.* **21**(2), 73–93 (2018)
- Edge, M., Allen, N.S., Gonzalez-Sanchez, R., Liauw, C.M., Read, S.J., Whitehouse, R.B.: The influence of cure and carbon black on the high temperature oxidation of natural rubber I. Correlation of physico-chemical changes. *Polym. Degrad. Stabil.* **64**, 197–205 (1998)
- Celina, M., Gillen, K.T.: Advances in exploring mechanistic variations in thermal aging of polymers. In: Martin, J.W., Rynntz, R.A., Chin, J., Dickie, R.A. (eds.) *Service Life Prediction of Polymeric Materials*, pp. 45–56. Springer, Boston (2009)
- Herzig, A., Johlitz, M., Lion, A.: Experimental investigation on the consumption of oxygen and its diffusion into elastomers during the process of ageing. In: *Proceedings of the 9th European Conference on Constitutive Models for Rubber (ECCMR)*, vol. 9, pp. 23–28 (2015)
- Johlitz, M.: Zum Alterungsverhalten von Polymeren: Experimentell gestützte, thermo-chemomechanische Modellbildung und numerische Simulation. Universität der Bundeswehr München, Fakultät für Luft- und Raumfahrttechnik (2016)
- Broudin, M., Marco, Y., Le Saux, V., Charrier, P., Hervouet, W., Le Gac, P.Y.: Investigation of thermo-oxidative ageing effects on the fatigue design of automotive anti-vibration parts. In: *MATEC Web of Conferences* (2018)

15. Musil, B.: Ein Beitrag zur experimentell gestützten Modellierung der chemo-thermomechanischen Alterung von Nitrilkautschuk. Universität der Bundeswehr München (2020)
16. Newton, R.G.: Mechanism of exposure-cracking of rubbers. With a review of the influence of ozone. *Rubber Chem. Technol.* **18**(3), 504–556 (1945)
17. Braden, M., Gent, A.: The attack of ozone on stretched rubber vulcanizates. II. Conditions for cut growth. *J. Appl. Polym. Sci.* **3**(7), 100–106 (1960)
18. Braden, M., Gent, A.: The attack of ozone on stretched rubber vulcanizates. III. Actions of antiozonants. *J. Appl. Polym. Sci.* **6**(22), 449–455 (1962)
19. Andrews, E.H., Braden, M.: The reaction of ozone with surfaces of natural rubber, and its dependence upon strain. *J. Polym. Sci.* **55**(162), 787–798 (1961)
20. Andrews, E.H., Braden, M.: The surface reaction of ozone with chemically protected rubber. *J. Appl. Polym. Sci.* **7**(3), 1003–1013 (1963)
21. Lake, G.J.: Ozone cracking and protection of rubber. *Rubber Chem. Technol.* **43**(5), 1230–1254 (1970)
22. Clough, R.L., Gillen, K.T.: Polymer degradation under ionizing radiation: the role of ozone. *J. Polymer Sci. Polymer Chem.* **27**(7), 2313–2324 (1989). <https://doi.org/10.1002/pola.1989.080270715>
23. Criegee, R.: Mechanism of ozonolysis. *Angew. Chem. Int. Edition* **14**(11), 745–752 (1975)
24. Huntink, N.M., Datta, R.N., Noordermeer, J.W.M.: Addressing durability of rubber compounds. *Rubber Chem. Technol.* **77**(3), 476–511 (2004)
25. Ignatz-Hoover, F., To, B.H., Datta, R.N., De Hoog, A.J., Huntink, N.M., Talma, A.G.: Chemical additives migration in rubber. *Rubber Chem. Technol.* **76**(3), 747–768 (2003)
26. Lewis, P.M.: Effect of ozone on rubbers: countermeasures and unsolved problems. *Polym. Degrad. Stabil.* **15**(1), 33–66 (1986)
27. Gillen, K.T., Bernstein, R., Celina, M.: Die Herausforderungen beschleunigter Alterungsverfahren für die Vorhersage der Elastomerlebensdauer - Teil 1. *Gummi Fasern Kunstst* (2016)
28. Bundesumweltamt.: Aktuelle Luftdaten. www.umweltbundesamt.de/daten/luft/luftdaten/karten. Accessed 16 Nov 2021
29. Bayerisches Landesamt für Umwelt (LfU): Faktenblatt Ozon. Bürgermeister-Ulrich-Straße 160, 86179 Augsburg. www.lfu.bayern.de. Accessed 16 Nov 2021
30. United States Environmental Protection Agency.: Ground-level Ozone Basics [Webpage]. <https://www.epa.gov/ground-level-ozone-pollution/ground-level-ozone-basics>
31. Gillen, K.T., Celina, M., Bernstein, R.: Validation of improved methods for predicting long-term elastomeric seal lifetimes from compression stress–relaxation and oxygen consumption techniques. *Polym. Degrad. Stabil.* **82**(1), 25–35 (2003)
32. Tamm, U.: Beseitigung von organischen Schadstoffen in Abgasen durch Oxidation mit Ozon. Martin-Luther-Universität Halle-Wittenberg (2002)
33. DIN ISO 1431-1. Elastomere oder thermoplastische Elastomere-Widerstand gegen Ozonrissbildung -Teil 1: Statische und dynamische Dehnungsprüfung. DIN Deutsches Institut für Normung e. V. (2017)
34. Gillen, K.T., Clough, R.L., Quintana, C.A.: Modulus profiling of polymers. *Polym. Degrad. Stabil.* **17**(1), 31–47 (1987)
35. Geels, K., Fowler, D.B., Kopp, W.U., Rückert, M.: Metallographic and materialographic specimen preparation, light microscopy, image analysis, and hardness testing. vol. 46. ASTM international West Conshohocken (2007)
36. Hummel, D.O.: Atlas der Kunststoffanalyse. Hanser (1968)